Physics Letters A ••• (••••) •••–•••

Contents lists available at ScienceDirect

Physics Letters A

www.elsevier.com/locate/pla

Effects of nitrogen-doping configurations with vacancies on conductivity in graphene

T.M. Radchenko [a,*], V.A. Tatarenko [a], I.Yu. Sagalianov [b], Yu.I. Prylutskyy [b]

[a] Department of Solid State Theory, G.V. Kurdyumov Institute for Metal Physics of NASU, 36 Acad. Vernadsky Blvd., Kyiv, Ukraine
[b] Taras Shevchenko National University of Kyiv, 64 Volodymyrska Str., Kyiv, Ukraine

ARTICLE INFO

Article history:
Received 10 May 2014
Received in revised form 18 May 2014
Accepted 20 May 2014
Available online xxxx
Communicated by V.M. Agranovich

Keywords:
Graphene
Quantum transport
Point defects

ABSTRACT

We investigate electronic transport in the nitrogen-doped graphene containing different configurations of point defects: singly or doubly substituting N atoms and nitrogen–vacancy complexes. The results are numerically obtained using the quantum-mechanical Kubo–Greenwood formalism. Nitrogen substitutions in graphene lattice are modelled by the scattering potential adopted from the independent self-consistent *ab initio* calculations. Variety of quantitative and qualitative changes in the conductivity behaviour are revealed for both graphite- and pyridine-type N defects in graphene. For the most common graphite-like configurations in the N-doped graphene, we also consider cases of correlation and ordering of substitutional N atoms. The conductivity is found to be enhanced up to several times for correlated N dopants and tens times for ordered ones as compared to the cases of their random distributions. The presence of vacancies in the complex defects as well as ordering of N dopants suppresses the electron–hole asymmetry of the conductivity in graphene.

1. Introduction

Among the currently known and already experimentally implemented or prospective substitutional dopants in graphene films (*e.g.*, B [1–7], N [5–14], Al–S [15–17], Sc–Zn [18–21], Pt [21,22], Au [21,22], Bi [23]), nitrogen (along with boron) is an archetypical natural candidate because its incorporation in graphene lattice requires minor structural perturbations due to its atomic size close to C. The N doping offers an effective way to tailor the properties of graphene and thereby makes it a promising material for applications in field-effect transistor devices, solar and fuel cells, lithium ion batteries, ultracapacitors, biosensing, field emission, transparent electrodes, or high-performance photocatalysts (see Ref. [24] and references therein).

A series of experiments on structural variety of N-related defects in graphene [6–11] showed that its rich electronic properties are dependent on how the N-doping configurations are formed: as single (Fig. 1(a)) or double (Figs. 1(b)–1(d)) substitutions or as nitrogen–vacancy complexes comprising monovacancies (Figs. 1(e), 1(f), 1(h)) or divacancies (Fig. 1(g)). Single and double substitutions give rise to the electron-donor-like states and then to *n*-type doping, while complex defects with vacancies exhibit a hole-acceptor-like character, *i.e.* *p*-type doping [6,9,10]. Both graphite- and pyridine-type defects in Fig. 1 can be observed in graphene films, which are fabricated by chemical vapour deposition growth on different substrates [7,9,11]. Formation-energy calculations [12] indicate that graphitic defects in Fig. 1(a) are energetically favoured (stable) among the possible N-doping configurations in Fig. 1. Pyridine-like configurations in Figs. 1(e)–1(h) have higher formation energy, but are stable in the presence of both doping N atoms and vacancies attracting each other and increasing probability of their mutual generation [13]. The first numerical study of charge transport in N-doped graphene [25] deals with the most simple case of random distribution of singly substituting N atoms (Fig. 1(a)). However, in order to regulate the transport properties of graphene by chemical N-doping, it is important to consider all configurations of the N-related defects currently revealed in experiments.

In a given paper, we report on how such diverse N-doping configurations affect the conductivity in single-layer graphene sheet, using an exact numerical technique based on the Kubo–Greenwood formalism appropriate for realistic samples with millions of atoms (the size of our computational domain is 1 700 000 sites that corresponds to 210×210 nm^2). We also focus on random, correlated, and ordered distributions of N dopants in one of the most common doping configurations, which is found [10] to be singly substituting N atom in Fig. 1(a).

* Corresponding author.
E-mail address: tarad@imp.kiev.ua (T.M. Radchenko).

http://dx.doi.org/10.1016/j.physleta.2014.05.022
0375-9601/

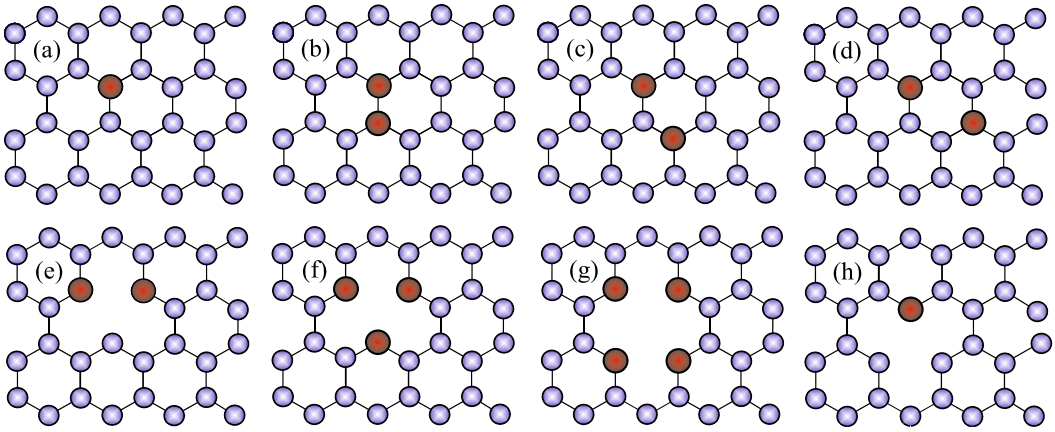

Fig. 1. (Colour online.) (a)–(d) Graphite- (substitutional) and (e)–(h) pyridine-type defects in graphene lattice. N atoms substitute C ones (a) singly, (b)–(d) doubly or form complex (e) dimerized, (f) trimerized, (g) tetramerized, or (h) monomeric defects with vacancies. Doubly substituting N atoms belong to the same sublattice (c) or different ones (b), (d).

2. Tight-binding model along with Kubo–Greenwood formalism

To investigate charge transport in the N-doped graphene, a real-space numerical implementation within the Kubo–Greenwood formalism [26,27], which captures all (ballistic, diffusive, and localization) transport regimes, is employed. Within this approach, the energy (E) and time (t) dependent transport coefficient, $D(E,t)$ [30], is governed by the wave-packet propagation [26,27]: $D(E,t) = \langle \Delta\hat{X}^2(E,t)\rangle/t$, where the mean quadratic spreading of the wave packet along the direction x reads as [26,27]

$$\left\langle \Delta\hat{X}^2(E,t)\right\rangle = \frac{\mathrm{Tr}[(\hat{X}(t)-\hat{X}(0))^2\delta(E-\hat{H})]}{\mathrm{Tr}[\delta(E-\hat{H})]} \tag{1}$$

with $\hat{X}(t) = \hat{U}^\dagger(t)\hat{X}\hat{U}(t)$—the position operator in the Heisenberg representation, $\hat{U}(t) = e^{-i\hat{H}t/\hbar}$—the time-evolution operator, and a standard p-orbital nearest-neighbour tight-binding Hamiltonian $\hat{H}$ is [28,29]

$$\hat{H} = -u\sum_{i,i'} c_i^\dagger c_{i'} + \sum_i V_i c_i^\dagger c_i, \tag{2}$$

where $c_i^\dagger$ (c_i) is a standard creation (annihilation) operator acting on a quasiparticle at the site i. The summation over i runs the entire honeycomb lattice, while i' is restricted to the sites next to i; $u = 2.7$ eV is the hopping integral for the neighbouring C atoms occupying i and i' sites at a distance $a = 0.142$ nm between them; and V_i is the on-site potential describing scattering by the N dopants.

The impurity scattering potential in the Hamiltonian matrix is introduced as on-site energies V_i varying with distance r to the impurity N atom at the site i according to the potential profile $V = V(r) < 0$ in Fig. 2 adopted from the self-consistent *ab initio* calculations [31]. As fitting shows, this potential is far from the Coulomb- or Gaussian-like shapes commonly used in the literature for charged impurities in graphene, while two-exponential fitting exactly reproduces the potential. Such a scattering potential presents both short-range and some long-range features [25]. A vacancy can be regarded as a site with hopping parameters to other sites being zero (note that another way to model vacancy at the site i is $V_i \to \infty$) [32]. In our numerical simulations, we implement a vacancy removing the atom at the vacancy site.

The dc conductivity σ can be extracted from the diffusivity $D(E,t)$, when it saturates reaching the maximum value, $\lim_{t\to\infty} D(E,t) = D_{\max}(E)$, and the diffusive transport regime occurs. Then the semiclassical conductivity at a zero temperature is defined as [26,27]

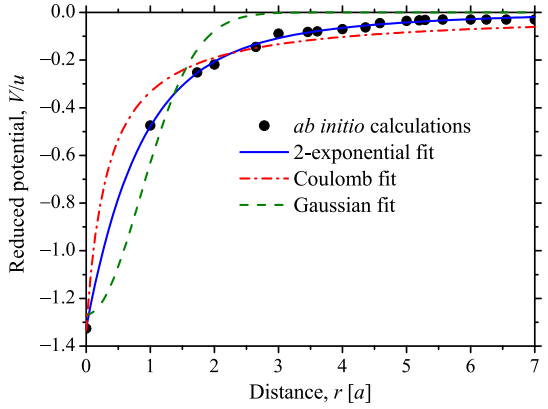

Fig. 2. (Colour online.) Scattering potential (•) adopted from Ref. [31] and fitted by different functions: Gaussian-like ($V = Ue^{-r^2/2\xi^2}$ with fitting parameters $U = -1.27u$ and $\xi = 0.85a$ standing here as a maximal potential height and an effective potential radius, respectively), Coulomb-like ($V = U/(\xi + r)$ with $U = -0.44ua$ and $\xi = 0.33a$), and two-exponential ($V = U_1e^{-r/\xi_1} + U_2e^{-r/\xi_2}$ with $U_1 = -1.07u$, $\xi_1 = 0.79a$, $U_2 = -0.25u$, $\xi_2 = 2.72a$).

$$\sigma = e^2\tilde{\rho}(E)D_{\max}(E), \tag{3}$$

where $-e < 0$ denotes the electron charge and $\tilde{\rho}(E) = \rho/\Omega = \mathrm{Tr}[\delta(E-\hat{H})]/\Omega$ is the density of sates (DOS) per unit area Ω (and per spin). The DOS is also used to calculate the electron density as $n_e(E) = \int_{-\infty}^{E}\tilde{\rho}(E)dE - n_{\mathrm{ions}}$, where $n_{\mathrm{ions}} = 3.9\cdot 10^{15}$ cm^{-2} is the density of the positive ions in the graphene lattice compensating the negative charge of the p-electrons (at the neutrality (Dirac) point of pristine graphene, $n_e(E) = 0$). Combining the calculated $n_e(E)$ with $\sigma(E)$, we compute the density dependence of the conductivity $\sigma = \sigma(n_e)$.

Note that we do not go into details of numerical calculations of DOS, $D(E,t)$, and σ since details of the computational method we utilize here (Chebyshev method for solution of the time-dependent Schrödinger equation, calculation of the first diagonal element of the Green's function using continued fraction technique and tridiagonalization procedure of the Hamiltonian matrix, averaging over the N and vacancy realizations, sizes of initial wave packet and computational domain, boundary conditions, etc.) are given in Ref. [27].

3. Results and discussion

Fig. 3 demonstrates the electron-density dependent conductivity for defect configurations depicted in Fig. 1. To compare conduc-